Universality in few-body systems with large scattering length

H.-W. Hammer

Institute for Nuclear Theory, University of Washington, Seattle, WA 98195-1550, USA

Abstract. Effective Field Theory (EFT) provides a powerful framework that exploits a separation of scales in physical systems to perform systematically improvable, model-independent calculations. Particularly interesting are few-body systems with short-range interactions and large two-body scattering length. Such systems display remarkable universal features. In systems with more than two particles, a three-body force with limit cycle behavior is required for consistent renormalization already at leading order. We will review this EFT and some of its applications in the physics of cold atoms and nuclear physics. In particular, we will discuss the possibility of an infrared limit cycle in QCD. Recent extensions of the EFT approach to the four-body system and N-boson droplets in two spatial dimensions will also be addressed.

Keywords: Effective field theory, universality, limit cycle
PACS: 03.70.+k, 03.75.-b, 12.38.Aw, 21.45.+v

INTRODUCTION

A separation of scales in a physical system can be exploited using the framework of Effective Field Theory (EFT) [1]. In EFT, only low-energy (or long-range) degrees of freedom are included explicitly, while all others are parametrized in terms of the most general local contact interactions. This approach relies on the fact that a low-energy probe of momentum k cannot resolve structures on scales smaller than $1/k$. (Note that $\hbar = c = 1$ in this talk.) As a consequence, the influence of short-distance physics on low-energy observables can be captured in a few low-energy constants. The EFT describes universal low-energy physics independent of detailed assumptions about the short-distance dynamics.

All low-energy observables can be calculated in a controlled expansion in powers of kl, where l is the characteristic low-energy length scale of the system. Error estimates can be obtained from the higher orders in the expansion in kl. The size of l depends on the system under consideration: for particles interacting via a finite range potential, e.g., l is given by the range of the potential. For the examples discussed in this talk, l is of the order of the effective range r_e.

We will focus on applications of EFT to few-body systems with large S-wave scattering length $|a| \gg l$. For a generic system, the scattering length is of the same order of magnitude as the low-energy length scale l. Only a very specific choice of the parameters in the underlying theory (a so-called *fine tuning*) will generate a large scattering length a. Nevertheless, systems with large a can be found in many areas of physics. The fine tuning can be accidental or it can be controlled by an external parameter.

Examples with an accidental fine tuning are the S-wave scattering of nucleons and of ^{4}He atoms. For S-wave nucleon-nucleon scattering, the scattering lengths and effective ranges are $a_s = -23.76$ fm and $r_s = 2.75$ fm in the spin-singlet channel and $a_t = 5.42$ fm and $r_t = 1.76$ fm in the spin-triplet channel. The effective ranges are both comparable to the characteristic low-energy length scale $\ell_\pi = 1/m_\pi \approx 1.4$ fm which is given by the inverse pion mass. However the scattering length a_s is much larger than ℓ_π and a_t is at least significantly larger. For ^{4}He atoms, the scattering length $a \approx 104$Å is more than a factor 10 larger than the typical low-energy length scale $l \approx 5$Å given by the van der Waals interaction. The scattering length of alkali atoms close to a Feshbach resonance can be tuned experimentally by adjusting the external magnetic field. In Fig. 1, we show the scattering length of ^{85}Rb atoms as a function of the magnetic field near the Feshbach resonance at $B = 155$ G. Sufficiently close to the resonance, the scattering length can be made arbitrarily large.

At very low energies all these systems behave similarly and show universal properties associated with the large scattering length. A simple example in the two-body sector for $a > 0$ is the existence of a shallow molecule (the *dimer*) with binding energy $B_2 = 1/(ma^2)$. A particularly remarkable example in the three-body sector is the existence of shallow three-body bound states (*Efimov states*) with universal properties [2]. Efimov states can cause dramatic dependence of scattering observables on a and on the energy [3, 4].

We are interested in processes with typical momenta $k \sim 1/|a|$. In this case, the EFT expansion becomes an expansion in powers of $l/|a|$. In leading order, we can simply set $l = 0$ and three-body observables are determined by a and by a three-body parameter that also determines the Efimov spectrum. The higher-order corrections in $l/|a|$ can

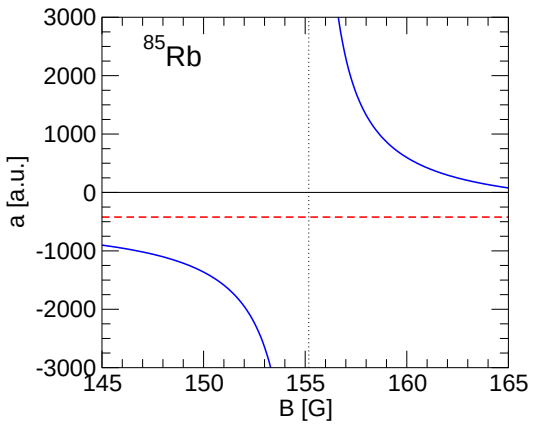

FIGURE 1. The scattering length a of ^{85}Rb atoms (in atomic units) as a function of the magnetic field close to the Feshbach resonance at $B = 155$ G (solid line). The dashed line indicates the off-resonant value of a, while the vertical dotted line gives the resonance position.

be calculated but will not be discussed in detail in this talk.

In the next section, we will briefly review the EFT for three-body systems with large scattering length a. In the following sections, we will discuss some applications in nuclear and atomic physics. In particular, we will discuss the possibility of an infrared limit cycle in QCD. Recent extensions of the EFT approach to the four-body system and N-boson droplets in two spatial dimensions will also be addressed. For a more detailed review, see Ref. [4].

THREE-BODY SYSTEM WITH LARGE SCATTERING LENGTH

We start with with a two-body system of nonrelativistic bosons with large S-wave scattering length a and mass m. The generalization to fermions is straightforward but will not be discussed in detail. In the following, we will refer to the bosons simply as atoms. At sufficiently low energies, the most general Lagrangian may be written as:

$$\mathscr{L} = \psi^\dagger \left(i\partial_t + \frac{\vec{\nabla}^2}{2m} \right) \psi - \frac{g_2}{4}(\psi^\dagger\psi)^2 - \frac{g_3}{36}(\psi^\dagger\psi)^3 + \dots , \tag{1}$$

where the dots represent higher-order derivative terms which are suppressed at low energies. The strength of the two-body interaction g_2 is determined by the scattering length a, while the three-body interaction g_3 depends on a parameter to be introduced below. For momenta k of the order of the inverse scattering length $1/|a|$, the problem is nonperturbative in ka. The full two-atom scattering amplitude can be obtained analytically by summing the so-called *bubble diagrams* with the g_2 interaction term shown in Fig. 2. The g_3 term does not contribute to two-body

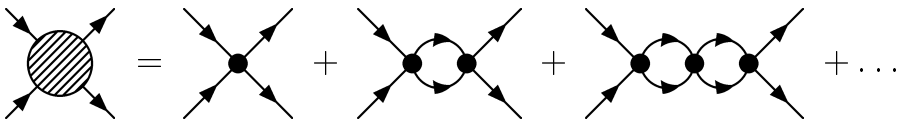

FIGURE 2. The bubble diagrams with the g_2 interaction contributing to the two-body scattering amplitude.

observables. The bubble diagrams are ultraviolet divergent and have to be regulated. This can be done by introducing an ultraviolet cutoff Λ in the loop integrals. The atom-atom scattering amplitude f_{AA} can be renormalized by allowing the coupling g_2 to depend on Λ and choosing $g_2(\Lambda)$ such that f_{AA} is independent of the regulator. After renormalization, the resulting amplitude reproduces the leading order of the well-known effective range expansion for the scattering amplitude: $f_{AA}(k) = (-1/a - ik)^{-1}$, where the total energy is $E = k^2/m$ and k is the center-of-mass momentum. If $a > 0$, f_{AA} has a pole at $k = i/a$ corresponding to a shallow dimer with binding energy $B_2 = 1/(ma^2)$. Higher-order derivative interactions are perturbative and give the momentum-dependent terms in the effective range expansion.

We now turn to the three-body system. At leading order in $l/|a|$, the atom-dimer scattering amplitude is given by the integral equation shown in Fig. 3. A solid line indicates the single-atom propagator and a double line indicates

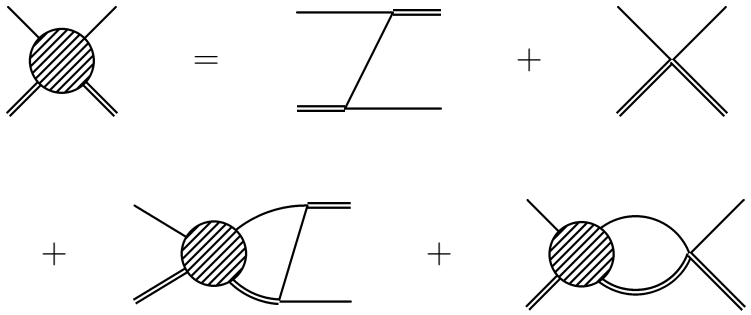

FIGURE 3. The integral equation for the atom-dimer scattering amplitude. The single (double) line indicates the single-atom (two-atom) propagator.

the full two-body propagator including all atom bubbles (cf. Fig. 2). The integral equation contains contributions from both the two-body and the three-body interaction terms g_2 and g_3, respectively. The inhomogeneous term is given by the first two diagrams on the right-hand side: the one-atom exchange diagram and the contribution of the three-body interaction. The integral equation simply sums these diagrams to all orders. After projecting onto S-waves, we obtain the equation

$$\mathscr{T}(k,p;E) \;=\; \frac{16}{3a}M(k,p;E)+\frac{4}{\pi}\int_0^\Lambda \frac{dq\,q^2 M(q,p;E)\,\mathscr{T}(k,q;E)}{-1/a+\sqrt{3q^2/4-mE-i\varepsilon}}\,, \tag{2}$$

for the off-shell atom-dimer scattering amplitude with the inhomogeneous term

$$M(k,p;E) \;=\; \frac{1}{2pk}\ln\left(\frac{p^2+pk+k^2-mE}{p^2-pk+k^2-mE}\right)+\frac{H(\Lambda)}{\Lambda^2}\,. \tag{3}$$

The logarithmic term is the S-wave projected one-atom exchange, while the term proportional to $H(\Lambda)$ comes from the three-body interaction. Note that we have introduced a cutoff regulator Λ in Eq. (2). This cutoff is required to insure that (2) has a unique solution. It is convenient to express g_3 as

$$g_3 = -\frac{9g_2^2}{\Lambda^2}H(\Lambda)\,, \tag{4}$$

which defines the function $H(\Lambda)$ in Eq. (3). The S-wave atom-dimer scattering amplitude f_{AD} is given by the solution $\mathscr{T}$ of Eq. (2) evaluated at the on-shell point:

$$f_{AD}(k) = \frac{1}{k\cot\delta_0 - ik} = \mathscr{T}(k,k;E)\,, \qquad \text{where} \qquad E=\frac{3k^2}{4m}-\frac{1}{ma^2} \tag{5}$$

is the total energy and k is the center-of-mass momentum. The three-body binding energies B_3 are given by those values of $E<0$ for which the homogeneous version of Eq. (2) has a nontrivial solution.

All physical observables must be independent of the regulator Λ. Therefore, we can determine $H(\Lambda)$ by varying Λ and demanding invariance of the low-energy three-body observables under this renormalization group transformation. This leads to the expression [5, 6]:

$$H(\Lambda) = \frac{\cos[s_0\ln(\Lambda/\Lambda_*)+\arctan s_0]}{\cos[s_0\ln(\Lambda/\Lambda_*)-\arctan s_0]}\,, \tag{6}$$

where $s_0 = 1.00624...$ is a solution to the transcendental equation

$$s_0\cosh\frac{\pi s_0}{2} = \frac{8}{\sqrt{3}}\sinh\frac{\pi s_0}{6}\,, \tag{7}$$

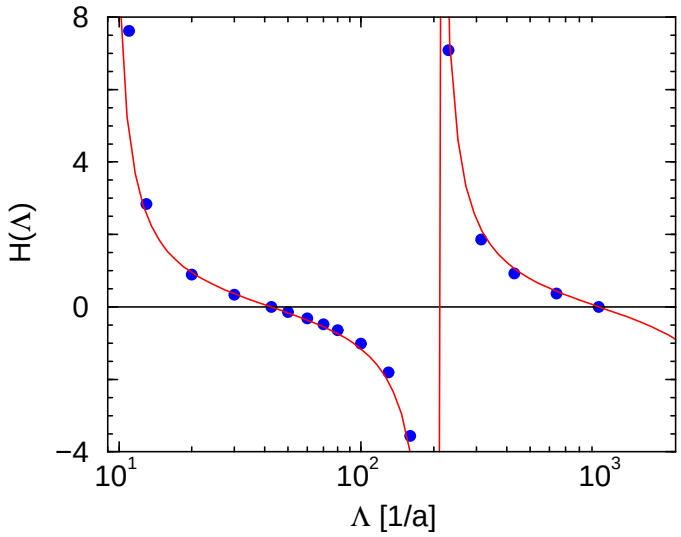

FIGURE 4. The three-body coupling H as a function of the cutoff Λ for a fixed value of the three-body parameter Λ_*. The solid line shows the analytical expression (6), while the dots show results from the numerical solution of Eq. (2).

and Λ_* is a three-body parameter introduced by dimensional transmutation. This parameter cannot be predicted by the EFT and must be determined from a three-body observable. The dependence of the three-body coupling H on the cutoff Λ is shown in Fig. 4 for a fixed value of the three-body parameter Λ_*. The solid line shows the analytical expression (6), while the dots show results from the numerical solution of Eq. (2). A good agreement between both methods is observed, indicating that the renormalization of Eq. (2) is well under control. Note that $H(\Lambda)$ is periodic and runs on a limit cycle. An important signature of an renormalization group (RG) limit cycle is discrete scale invariance. When Λ is increased by a factor of $\exp(\pi/s_0) \approx 22.7$, $H(\Lambda)$ returns to its original value. Discrete scale invariance also arises in other contexts as varied as turbulence, sandpiles, earthquakes, and financial crashes [7]. The possibility of renormalization group limit cycles was first pointed out by Wilson in 1971 [8], but no explicit examples were known at the time. Recently, a number of field-theoretical models with limit cycles have been constructed [9, 10, 11, 12]. Leclair, Roman, and Sierra have used the colorful phrase *Russian doll renormalization group* to describe RG limit cycles [11, 12]. The name refers to a traditional souvenir from Russia consisting of a set of hollow wooden dolls that can be nested inside each other. Similar to a limit cycle, the dolls show discrete scale invariance: the scaling factors between each doll and the next smaller one are all approximately equal.

In summary, two parameters are required to specify a three-body system with large scattering length at leading order in $l/|a|$: they may be chosen as the scattering length a (or equivalently B_2 if $a > 0$) and the three-body parameter Λ_* [5, 6]. In the following sections, we will discuss some applications of this EFT in nuclear and atomic physics.

UNIVERSAL PROPERTIES OF FEW-BODY SYSTEMS

This EFT confirms and extends the universal predictions for the three-body system first derived by Efimov [2, 3]. The best known example is the *Efimov effect*, the accumulation of infinitely-many three-body bound states at threshold as $a \to \pm\infty$ [2]. The ratio of the binding energies of successively shallower states rapidly approaches a constant $\lambda_0^2 = \exp(2\pi/s_0) \approx 515$.

However, universality also constrains three-body scattering observables. The atom-dimer scattering length, e.g., can be expressed in terms of a and Λ_* as [3, 13]

$$a_{12} = a\,(1.46 - 2.15\tan[s_0\ln(a\Lambda_*) + 0.09])\,(1 + \mathcal{O}(l/a))\,, \qquad a > 0\,. \tag{8}$$

Note that the log-periodic dependence of H on Λ_* is not an artefact of the renormalization and is also manifest in observables like a_{12}. This dependence could, e.g., be tested experimentally with atoms close to a Feshbach resonance by varying a. Similar expressions can be obtained for other three-body observables such as scattering phase shifts

as well as rates for three-body recombination and dimer relaxation (including the effects of deeply-bound two-body states) [14].

Since up to corrections of order $l/|a|$, low-energy three-body observables depend on a and Λ_* only, they obey non-trivial scaling relations. If dimensionless combinations of such observables are plotted against each other, they must fall close to a line parametrized by Λ_* [6, 13]. An example of a scaling function relating ^{4}He trimer ground and excited state energies $B_3^{(0)}$ and $B_3^{(1)}$ is shown in the left panel of Fig. 5. (A related scaling function was obtained in

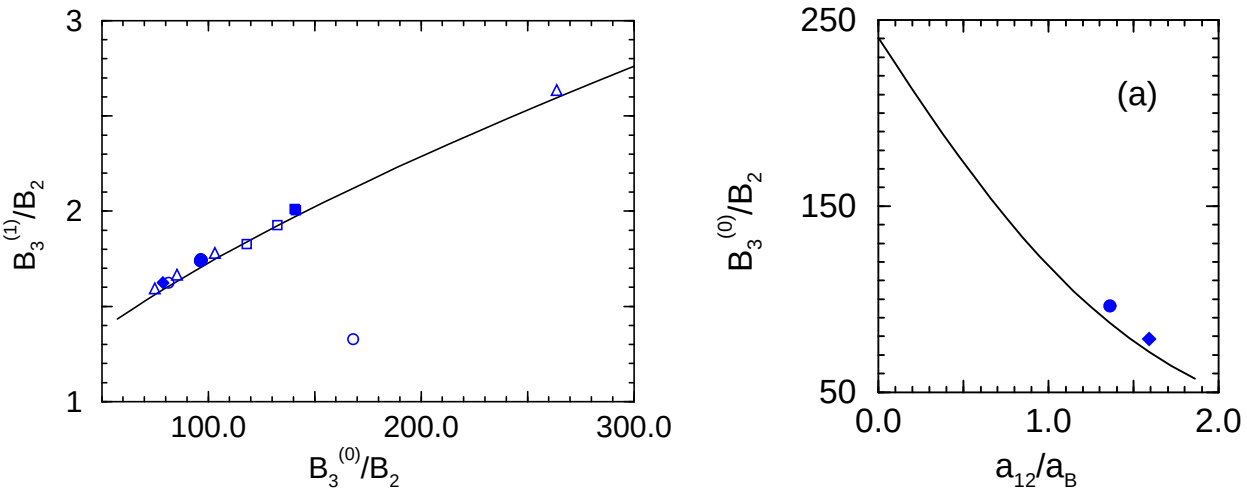

FIGURE 5. The scaling functions relating the ^{4}He trimer ground and excited state energies (left panel) and the ^{4}He trimer ground state and the atom-dimer scattering length (right panel). The data points are calculations using various methods and ^{4}He potentials (see Ref. [16] and references therein). Note that $a_B \equiv 1/\sqrt{mB_2}$.

Ref. [15].) The data points show calculations using various approaches and ^{4}He potentials. Since different potentials have approximately the same scattering length but include different short-distance physics, different points on this line correspond to different values of Λ_*. The small deviations of the potential model calculations are mainly due to effective range effects. They are of the order $r_e/a \approx 10\%$ and can be calculated at next-to-leading order in EFT. The calculation corresponding to the data point far off the universal curve can easily be identified as problematic since the deviation from universality by far exceeds the expected 10%. The right panel shows the scaling function relating the ^{4}He trimer ground state energy $B_3^{(0)}$ and the atom-dimer scattering length a_{12}. A similar scaling relation is observed in nuclear physics between the spin-doublet neutron-deuteron scattering length and the triton binding energy and is known as the Phillips line [17].

Recently, we have extended the effective theory for large scattering length to the four-body system [18]. It is advantageous in this case to use an effective quantum mechanics framework, since one can start directly from the well-known Yakubovsky equations. We have shown that no four-body parameter enters at leading order in $l/|a|$. Therefore renormalization of the three-body system automatically guarantees renormalization of the four-body system. As a consequence, there are universal scaling functions relating three- and four-body observables as well. As an example, we show the correlation between the trimer and tetramer binding energies in Fig. 6. The left panel shows the correlation between the ground state energies while the right panel shows the correlation between the excited state energies. The data points are calculations using various methods and ^{4}He potentials (see Ref. [19] and references therein). We conclude that universality is well satisfied in the three- and four-body systems of ^{4}He atoms.

The existence of these scaling functions is a universal feature of systems with large scattering length and is independent of the details of the short-distance physics. Similar correlations between few-body observables appear for example also in nuclear systems. The correlation between the triton and α particle binding energies (the Tjon line [20]) and the Phillips line can be explained using a similar effective theory [21, 22, 23]. The spin-singlet and spin-triplet scattering lengths a_s and a_t for nucleons are both significantly larger than the range of the nuclear force. This observation can be used as the basis for an EFT approach to the few-nucleon problem in which the nuclear forces are approximated by contact interactions with strengths adjusted to reproduce the scattering lengths a_s and a_t [23]. (For an earlier related approach, see Ref. [24].) This EFT does not contain explicit pion degrees of freedom and is sometimes referred to as *pionless EFT*. The EFT involves an isospin doublet N of Pauli fields with two independent two-body contact interactions: $N^\dagger \sigma_i N^c N^{c\dagger} \sigma_i N$ and $N^\dagger \tau_k N^c N^{c\dagger} \tau_k N$, where $N^c = \sigma_2 \tau_2 N^*$. Renormalization in the two-

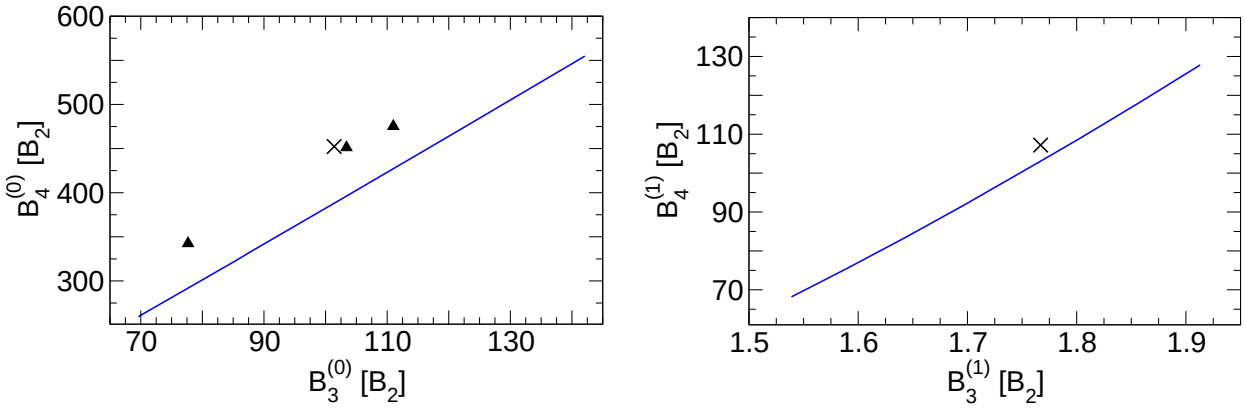

FIGURE 6. The scaling function relating the ^{4}He trimer and tetramer ground state (left panel) and excited state (right panel) energies. The data points are calculations using various methods and ^{4}He potentials (see Ref. [19] and references therein).

body sector requires the two coupling constants to be adjusted as functions of Λ to obtain the correct values of a_s and a_t. Renormalization in the three-body sector requires a three-body contact interaction $N^\dagger\sigma_i N^c N^{c\dagger}\sigma_j N N^\dagger\sigma_i\sigma_j N$ with a coupling constant proportional to (6) [23]. Thus the renormalization involves an ultraviolet limit cycle. The scaling-violation parameter Λ_* can be determined by using the triton binding energy B_t as input. Effective range effects and other higher order corrections can be treated in perturbation theory [25].

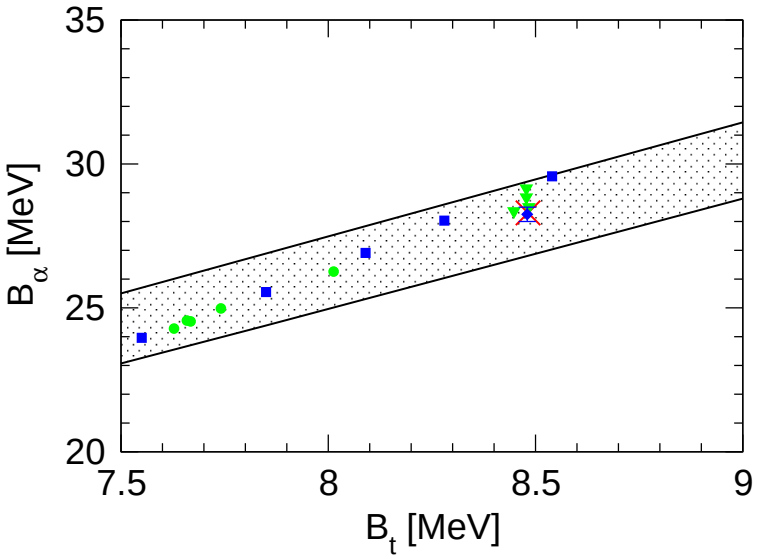

FIGURE 7. The correlation between the binding energies of the triton and the α particle (the Tjon line). The lower (upper) line shows our leading order result using a_s and B_d (a_s and a_t) as two-body input. The grey circles and triangles show various calculations using phenomenological potentials [26]. The squares show the results of chiral EFT at NLO for different cutoffs while the diamond shows the N^{2}LO result [27, 28]. The cross shows the experimental point.

In Fig. 7, we show the result for the Tjon line with a_s and B_d as input (lower line) and a_s and a_t as two-body input (upper line). Both lines generate a band that gives a naive estimate of higher order corrections in $\ell/|a|$. We also show some calculations using phenomenological potentials [26] and a chiral EFT potential with explicit pions [27, 28]. All calculations with interactions that give a large scattering length must lie close to this line. Different short-distance physics and/or cutoff dependence should only move the results along the Tjon line. This can for example be observed in the NLO results with the chiral potential indicated by the squares in Fig. 7 or in the few-body calculations with the low-momentum NN potential $V_{\text{low}-k}$ carried out in Ref. [29]. The $V_{\text{low}-k}$ potential is obtained from phenomenological NN interactions by intergrating out high-momentum modes above a cutoff Λ but leaving two-body observables (such

as the large scattering lengths) unchanged. The results of few-body calculations with $V_{\mathrm{low}-k}$ are not independent of Λ but lie all close to the Tjon line (cf. Fig. 2 in Ref. [29]).

If we take the triton binding energy $B_t = 8.48$ MeV as input, we can use the curves in Fig. 7 to predict the binding energy of the α particle. If the spin-singlet and spin-triplet scattering lengths a_s and a_t are used as the two-body input, we find $B_\alpha = 29.5$ MeV. If the deuteron binding energy B_d is used as input instead of a_t, we obtain $B_\alpha = 26.9$ MeV. This variation is consistent with the expected 30% accuracy of a leading order calculation in $\ell/|a|$. Our results agree with the (Coulomb corrected) experimental value $B_\alpha^{exp} = (29.0 \pm 0.1)$ MeV to within 10%. We conclude that the ground state energy of the α particle can be described by an effective theory with short-range interactions only. Of course, a more refined analysis should also include Coulomb corrections. However, the size of these corrections is expected to be smaller than the NLO contribution from the two-body effective ranges. Furthermore, corrections due to isospin violation will appear naturally at higher order within the effective theory.

AN INFRARED LIMIT CYCLE IN QCD

The low-energy few-nucleon problem can also be described by an EFT that includes explicit pion fields. Such an EFT has been used to extrapolate nuclear forces to the chiral limit of QCD in which the pion is exactly massless [30, 31, 32, 33]. In Fig. 8, we show the results for the extrapolation of the inverse scattering lengths $1/a_t$ and $1/a_s$ as functions of m_π from the calculation by Epelbaum et al. [33]. The extrapolation to larger values of m_π predicts

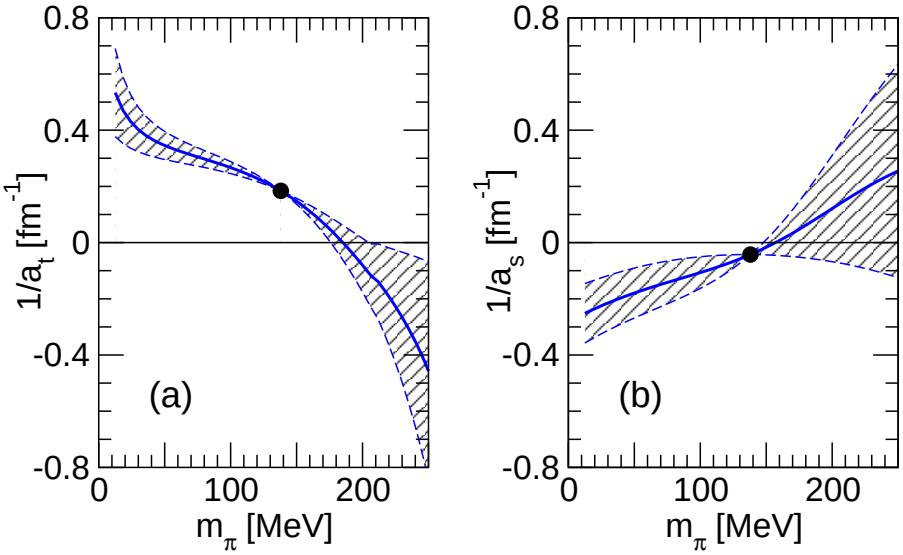

FIGURE 8. The inverse scattering lengths $1/a_t$ (left panel) and $1/a_s$ (right panel) as functions of m_π as predicted by the EFT with pions of Ref. [33].

that a_t diverges and the deuteron becomes unbound at a critical value in the range 170 MeV $< m_\pi <$ 210 MeV. It is also predicted that a_s is likely to diverge and the spin-singlet deuteron become bound at some critical value of m_π not much larger than 150 MeV. Both critical values are close to the physical value $m_\pi = 135$ MeV. Beane and Savage have argued that the errors in the extrapolation to the chiral limit are larger than estimated in Ref. [33], but their errors agree for the small extrapolation to the critical values [31, 32].

Chiral extrapolations can also be calculated using the EFT without pions [34]. The inputs required are the chiral extrapolations $a_s(m_\pi)$, $a_t(m_\pi)$, and $B_t(m_\pi)$, which can be calculated using an EFT with pions. As an illustration, we take the central values of the error bands for the inverse scattering lengths $1/a_s(m_\pi)$ and $1/a_t(m_\pi)$ from the chiral extrapolation in Ref. [33]. Since the chiral extrapolation of the triton binding energy $B_t(m_\pi)$ has not yet been calculated and since Λ_* should vary smoothly with m_π, we approximate it by its physical value $\Lambda_* = 189$ MeV for $m_\pi = 138$ MeV. In Fig. 9, we show the resulting three-body spectrum in the triton channel as a function of m_π. Near $m_\pi \approx 175$ MeV where the decay threshold comes closest to $\kappa = 0$, an excited state of the triton appears. This excited state is a hint that the system is very close to an infrared limit cycle. In the case illustrated by Fig. 9, the value of m_π at which

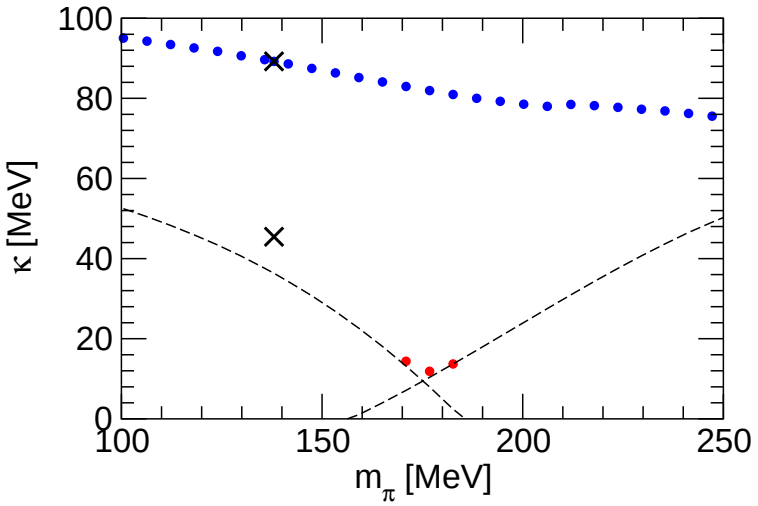

FIGURE 9. The binding momenta $\kappa = (mB_3)^{1/2}$ of *pnn* bound states as a function of m_π. The circles are the triton ground state and excited state. The crosses are the physical binding energies of the deuteron and triton. The dashed lines are the thresholds for decay into a nucleon plus a deuteron (left curve) or a spin-singlet deuteron (right curve).

a_t diverges is larger than that at which a_s diverges. If they both diverged at the same value of m_π, there would be an exact infrared limit cycle.

We conjecture that QCD can be tuned to this infrared limit cycle by adjusting the up and down quark masses m_u and m_d [34]. As illustrated in Fig. 9, the tuning of m_π, which corresponds to $m_u + m_d$, is likely to bring the system close enough to the infrared limit cycle for the triton to have one excited state. We conjecture that by adjusting the two parameters m_u and m_d to critical values, one can make a_t and a_s diverge simultaneously. At this critical point, the deuteron and spin-singlet deuteron would both have zero binding energy and the Efimov effect [2] would occur: the triton would have infinitely-many increasingly-shallow excited states. The ratio of the binding energies of successively shallower states would rapidly approach a constant λ_0^2 close to 515. The limit cycle would be manifest in the Efimov effect for the triton. This argument requires that QCD with the appropriate combination of up and down quark masses is in the same universality class as the three-body system with large scattering length [35]. It would be interesting to demonstrate the existence of this infrared RG limit cycle in QCD using Lattice QCD and EFT.

N-BOSON DROPLETS IN TWO DIMENSIONS

In this section, we consider the universal properties of weakly interacting bosons with large scattering length (or equivalently a shallow dimer state) in two spatial dimensions (2D) [36]. The 2D case is very different from the three-dimensional case discussed above. In particular, there is no Efimov effect or Thomas collapse and no three-body interaction is required at leading order. We consider self-bound droplets of $N(\gg 1)$ bosons interacting weakly via an *attractive*, short-ranged pair potential. (This corresponds to Eq. (1) with g_3 set to zero.) Our analysis relies strongly on the property of asymptotic freedom of 2D bosons with an attractive interaction.

In 2D, any attractive potential has at least one bound state. For the potential $-g\delta^2(r)$ with small $g > 0$, there is exactly one bound state with an exponentially small binding energy,

$$B_2 \sim \Lambda^2 \exp(-4\pi/g), \tag{9}$$

where Λ is the ultraviolet momentum cutoff (which is the inverse of the range of the potential). Asymptotic freedom provides an elegant way to understand this result. In 2D nonrelativistic theory, the four-boson interaction $g(\psi^\dagger\psi)^2$ is marginal. The coupling runs logarithmically with the length scale R, and the running can be found by performing the standard renormalization group (RG) procedure. For $g > 0$, the coupling grows in the infrared, in a manner similar to

the QCD coupling [37, 38]. The dependence of the coupling on the length scale R is given by

$$g(R) = \left[\frac{1}{g} - \frac{1}{4\pi}\ln(\Lambda^2 R^2)\right]^{-1}, \tag{10}$$

so the coupling becomes large when R is comparable to the size of the two body bound state $B_2^{-1/2}$. This is in essence the phenomenon of dimensional transmutation: a dynamical scale is generated by the coupling constant and the cutoff scale. It is natural, then, that B_2 is the only physical energy scale in the problem: the binding energy of three-particle, four-particle,... bound states are proportional to B_2. (Remember that in 2D there is no Efimov effect and no three-body parameter is required.) The N-particle binding energy B_N, however, can be very different from B_2 if N is parametrically large. We use the variational method to calculate the size of the bound state. For a cluster of a large number of bosons, one can apply classical field theory. We thus have to minimize the expectation value of the Hamiltonian with respect to all field configurations $\psi(r)$ satisfying the constraint $N = \int d^2 r\, \psi^\dagger \psi$. This is equivalent to a Hartree calculation with the running coupling constant $g(R)$ instead of the bare one. In the limit of a large number N of particles in the droplet, some exact predictions can be obtained.

The system possesses surprising universal properties. Namely, if one denotes the size of the N-body droplet as R_N, then at large N and in the limit of zero range of the interaction potential [36]:

$$\frac{R_{N+1}}{R_N} \approx 0.3417, \qquad \frac{B_{N+1}}{B_N} \approx 8.567, \qquad N \gg 1\,. \tag{11}$$

The size of the bound state decreases exponentially with N: adding a boson into an existing N-boson droplet reduces the size of the droplet by almost a factor of three. Correspondingly, the binding energy of N bosons B_N increases exponentially with N. This implies that the energy required to remove one particle from a N-body bound state (the analog of the nucleon separation energy for nuclei) is about 88% of the total binding energy. This is in contrast to most other physical systems, where separating one particle costs much less energy than the total binding energy, provided the number of particles in the bound state is large. Equations (11) are accurate to leading order in $1/N$ but the $1/N$-corrections are calculable.

For the universal predictions (11) to apply in realistic systems with finite-range interactions, the N-body bound states need to be sufficiently shallow and hence have a size R_N large compared to the natural low-energy length scale l. Depending on the physical system, l can be the van der Waals length, the range of the potential or some other scale. As a consequence, Eqs. (11) are valid in realistic systems for N large, but below a critical value,

$$1 \ll N \ll N_{\rm crit} \approx 0.931 \ln(R_2/l) + \mathcal{O}(1)\,. \tag{12}$$

At $N = N_{\rm crit}$ the size of the droplet is comparable to l and universality is lost. If there is an exponentially large separation between R_2 and l, then $N_{\rm crit}$ is much larger than one and the condition (12) can be satisfied.

We can compare our prediction with exact few-body calculations for $N = 3, 4$. While the $1/N$-corrections are expected to be relatively large in this case, we can estimate how the universal result for B_{N+1}/B_N is approached. The three-body system for a zero-range potential in 2D has exactly two bound states: the ground state with $B_3^{(0)} = 16.522688(1)\,B_2$ and one excited state with $B_3^{(1)} = 1.2704091(1)\,B_2$ [39, 40, 36]. Similarly, the four-body system for a zero-range potential in 2D has two bound states: the ground state with $B_4^{(0)} = 197.3(1)\,B_2$ and one excited state with $B_4^{(1)} = 25.5(1)\,B_2$ [41]. The prediction (11) applies to the ground state energies $B_3^{(0)}$ and $B_4^{(0)}$. The exact few-body results for $N = 3, 4$ are compared to the asymptotic prediction for B_N/B_{N-1} indicated by the dot-dashed line in Fig. 10. The ratio $B_3^{(0)}/B_2 \approx 16.5$ is almost twice as large as the asymptotic value (11), while the ratio $B_3^{(0)}/B_4^{(0)} \approx 11.9$ is already considerably closer. These deviations are expected for such small values of N. Note, however, that the ratio of the root mean square radii of the two- and three-body wave functions is 0.306 [40], close to the asymptotic value (11). The dashed line gives an estimate of how the large-N value should be approached [41]. This estimate assumes the expansion:

$$B_N = \left(c_0 + \frac{c_{-1}}{N} + \frac{c_{-2}}{N^2} + \ldots\right) 8.567^N, \tag{13}$$

leading to

$$\frac{B_N}{B_{N-1}} = 8.567 + \mathcal{O}\left(N^{-2}\right). \tag{14}$$

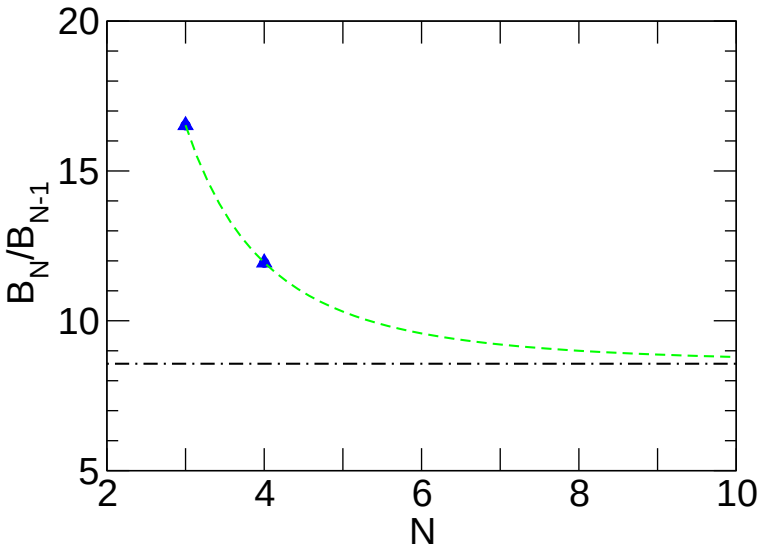

FIGURE 10. The ratio B_N/B_{N-1} as a function of N. The dot-dashed line shows the asymptotic value of 8.567. The dashed line is an estimate of how this value is approached as N increases.

The dashed line in Fig. 10 was obtained by fitting the coefficients of the $1/N^2$ and $1/N^3$ terms in Eq. (14) to the data points for $N = 3, 4$.

It would be interesting to test the universal predictions (11) both theoretically and experimentally for $N > 4$. On the theoretical side, Monte Carlo techniques appear to be a promising avenue. Furthermore, the experimental realizablity of self-bound 2D boson systems with weak interactions should be investigated. According to the estimate in Fig. 10, the $1/N$ corrections to Eqs. (11) are small for $N \gtrsim 6$. Using (12), this requires $R_2/\ell \gg 600$. We are not aware of any physical system that satisfies this constraint. However, such a system could possibly be realized close to a Feshbach resonance where R_2 can be made arbitrarily large.

SUMMARY

We have discussed the EFT for few-body systems with short-range interactions and large scattering length a. The renormalization of the three-body system with large a in three spatial dimensions requires a one-parameter three-body force governed by a limit cycle already at leading order in the expansion in $l/|a|$. As a consequence, two parameters are required to specify a three-body system: the scattering length a (or the dimer binding energy B_2) and the three-body parameter Λ_*. Once these two parameters are given, the properties of the three- and four-body systems are fully determined at leading order in $l/|a|$.

The large scattering length leads to universal properties independent of the short-distance dynamics. In particular, we have discussed universal expressions for three-body observables and universal scaling functions relating various few-body observables for both atomic and nuclear systems. A more detailed account including the effects of deeply-bound two-body states can be found in Ref. [4].

The success of the pionless EFT demonstrates that physical QCD is close to an infrared limit cycle. We have conjectured, that QCD could be tuned to the critical trajectory for the limit cycle by adjusting the up and down quark masses. The limit cycle would them be manifest in the Efimov effect for the triton [34]. It may be possible to demonstrate the existence of this infrared RG limit cycle in QCD using Lattice QCD and EFT.

In two spatial dimensions, the three-body parameter Λ_* does not enter at leading order in the expansion in $l/|a|$ and N-body binding energies only depend on B_2. The asymptotic freedom of non-relativistic bosons with attractive interactions in 2D leads to remarkable universal properties of N-body droplets, such as the exponential behavior of binding energies and droplet sizes in Eq. (11) [36].

The three-body effects discussed here will also become relevant in Fermi systems with three or more spin states. Future challenges include universality in the N-body problem for $N \geq 4$, effective range corrections, and a large

scattering length in higher partial waves. A large P-wave scattering length, for example, appears in nuclear Halo systems such as ^{6}He [42, 43].

ACKNOWLEDGMENTS

This work was done in collaboration with E. Braaten, U.-G. Meißner, L. Platter, and D.T. Son. It was supported in part by the US Department of Energy under grant DE-FG02-00ER41132. Local support from the organizers of the workshop on "Nuclei and Mesoscopic Physics" at NSCL at Michigan State University is gratefully acknowledged.

REFERENCES

1. See for example: D.B. Kaplan, arXiv:nucl-th/9506035; G.P. Lepage, arXiv:nucl-th/9706029.
2. V.N. Efimov, Sov. J. Nucl. Phys. **12**, 589 (1971).
3. V.N. Efimov, Sov. J. Nucl. Phys. **29**, 546 (1979).
4. E. Braaten and H.-W. Hammer, arXiv:cond-mat/0410417.
5. P.F. Bedaque, H.-W. Hammer, and U. van Kolck, Phys. Rev. Lett. **82**, 463 (1999) [arXiv:nucl-th/9809025].
6. P.F. Bedaque, H.-W. Hammer, and U. van Kolck, Nucl. Phys. A **646**, 444 (1999) [arXiv:nucl-th/9811046].
7. D. Sornette, Phys. Rep. **297**, 239 (1998) [arXiv:cond-mat/9707012].
8. K.G. Wilson, Phys. Rev. D **3**, 1832 (1971).
9. S. D. Glazek and K. G. Wilson, Phys. Rev. Lett. **89**, 230401 (2002) [arXiv:hep-th/0203088].
10. S. D. Glazek and K. G. Wilson, Phys. Rev. B **69**, 094304 (2004).
11. A. LeClair, J. M. Roman, and G. Sierra, Phys. Rev. B **69**, 20505 (2004) [arXiv:cond-mat/0211338].
12. A. Leclair, J. M. Roman, and G. Sierra, Nucl. Phys. B **675**, 584 (2003) [arXiv:hep-th/0301042].
13. E. Braaten and H.-W. Hammer, Phys. Rev. A **67**, 042706 (2003) [arXiv:cond-mat/0203421].
14. E. Braaten and H.-W. Hammer, Phys. Rev. A **70**, 042706 (2004) [arXiv:cond-mat/0303249].
15. T. Frederico, L. Tomio, A. Delfino, and A.E.A. Amorim, Phys. Rev. A **60**, R9 (1999).
16. A.K. Motovilov, W. Sandhas, S.A. Sofianos, and E.A. Kolganova, Eur. Phys. J. D **13**, 33 (2001).
17. A.C. Phillips, Nucl. Phys. A **107**, 209 (1968).
18. L. Platter, H.-W. Hammer, and U.-G. Meißner, Phys. Rev. A **70**, 052101 (2004) [arXiv:cond-mat/0404313].
19. D. Blume and C.H. Greene, J. Chem. Phys. **112**, 8053 (2000).
20. J.A. Tjon, Phys. Lett. B **56**, 217 (1975).
21. L. Platter, H.-W. Hammer, and U.-G. Meißner, Phys. Lett. B (in press) [arXiv:nucl-th/0409040].
22. V. Efimov and E.G. Tkachenko, Sov. J. Nucl. Phys. **47**, 17 (1988).
23. P.F. Bedaque, H.-W. Hammer, and U. van Kolck, Nucl. Phys. A **676**, 357 (2000) [arXiv:nucl-th/9906032].
24. V. Efimov, Nucl. Phys. A **362**, 45 (1981).
25. P.F. Bedaque, G. Rupak, H.W. Griesshammer, and H.-W. Hammer, Nucl. Phys. A **714**, 589 (2003) [arXiv:nucl-th/0207034], and references therein.
26. A. Nogga, H. Kamada, and W. Glöckle, Phys. Rev. Lett. **85**, 944 (2000) [arXiv:nucl-th/0004023].
27. E. Epelbaum, H. Kamada, A. Nogga, H. Witala, W. Glöckle, and U.-G. Meißner, Phys. Rev. Lett. **86**, 4787 (2001) [arXiv:nucl-th/0007057].
28. E. Epelbaum, A. Nogga, W. Glöckle, H. Kamada, U.-G. Meißner, and H. Witala, Phys. Rev. C **66**, 064001 (2002) [arXiv:nucl-th/0208023].
29. A. Nogga, S. K. Bogner, and A. Schwenk, Phys. Rev. C **70**, 061002 (2004) [arXiv:nucl-th/0405016].
30. S. R. Beane, P.F. Bedaque, M.J. Savage, and U. van Kolck, Nucl. Phys. A **700**, 377 (2002) [arXiv:nucl-th/0104030].
31. S. R. Beane and M. J. Savage, Nucl. Phys. A **713**, 148 (2003) [arXiv:nucl-th/0206113].
32. S. R. Beane and M. J. Savage, Nucl. Phys. A **717**, 91 (2003) [arXiv:nucl-th/0208021];
33. E. Epelbaum, U.-G. Meißner, and W. Glöckle, Nucl. Phys. A **714**, 535 (2003) [arXiv:nucl-th/0207089].
34. E. Braaten and H. W. Hammer, Phys. Rev. Lett. **91**, 102002 (2003) [arXiv:nucl-th/0303038].
35. K. G. Wilson, arXiv:hep-lat/0412043.
36. H.-W. Hammer and D.T. Son, Phys. Rev. Lett. **93**, 250408 (2004) [arXiv:cond-mat/0405206].
37. D. J. Gross and F. Wilczek, Phys. Rev. Lett. **30**, 1343 (1973).
38. H. D. Politzer, Phys. Rev. Lett. **30**, 1346 (1973).
39. L.W. Bruch, and J.A. Tjon, Phys. Rev. A **19**, 425 (1979).
40. E. Nielsen, D.V. Fedorov, and A.S. Jensen, Few-Body Syst. **27**, 15 (1999).
41. L. Platter, H.-W. Hammer, and U.-G. Meißner, Few-Body Syst. **35**, 169 (2004) [arXiv:cond-mat/0405660].
42. C.A. Bertulani, H.-W. Hammer, and U. van Kolck, Nucl. Phys. A **712**, 37 (2002) [arXiv:nucl-th/0205063].
43. P. F. Bedaque, H.-W. Hammer, and U. van Kolck, Phys. Lett. B **569**, 159 (2003) [arXiv:nucl-th/0304007].